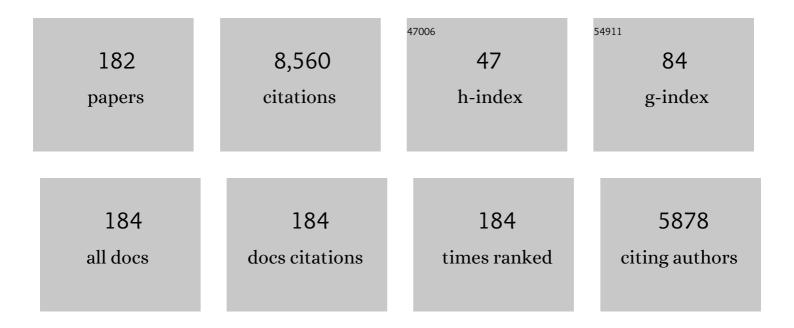
List of Publications by Year in descending order

Source: https://exaly.com/author-pdf/1904830/publications.pdf Version: 2024-02-01



#	Article	IF	CITATIONS
1	Antimony pollution in China. Science of the Total Environment, 2012, 421-422, 41-50.	8.0	466
2	Persulfate-based advanced oxidation processes (AOPs) for organic-contaminated soil remediation: A review. Chemical Engineering Journal, 2019, 372, 836-851.	12.7	435
3	Antimony speciation in the environment: Recent advances in understanding the biogeochemical processes and ecological effects. Journal of Environmental Sciences, 2019, 75, 14-39.	6.1	310
4	Distribution of polycyclic aromatic hydrocarbons in water, suspended particulate matter and sediment from Daliao River watershed, China. Chemosphere, 2007, 68, 93-104.	8.2	295
5	Adsorption of antimony onto iron oxyhydroxides: Adsorption behavior and surface structure. Journal of Hazardous Materials, 2014, 276, 339-345.	12.4	292
6	Distribution and phytoavailability of antimony at an antimony mining and smelting area, Hunan, China. Environmental Geochemistry and Health, 2007, 29, 209-219.	3.4	251
7	Removal of antimony(V) and antimony(III) from drinking water by coagulation–flocculation–sedimentation (CFS). Water Research, 2009, 43, 4327-4335.	11.3	241
8	Antimony distribution and mobility in rivers around the world's largest antimony mine of Xikuangshan, Hunan Province, China. Microchemical Journal, 2011, 97, 4-11.	4.5	202
9	Adsorption of antimony(III) and antimony(V) on bentonite: Kinetics, thermodynamics and anion competition. Microchemical Journal, 2011, 97, 85-91.	4.5	195
10	Heavy metal loss from agricultural watershed to aquatic system: A scientometrics review. Science of the Total Environment, 2018, 637-638, 208-220.	8.0	178
11	Heavy metal pollution of the world largest antimony mine-affected agricultural soils in Hunan province (China). Journal of Soils and Sediments, 2010, 10, 827-837.	3.0	166
12	Mechanisms of Sb(III) Oxidation by Pyrite-Induced Hydroxyl Radicals and Hydrogen Peroxide. Environmental Science & Technology, 2015, 49, 3499-3505.	10.0	144
13	Removal of antimony (III) and antimony (V) from drinking water by ferric chloride coagulation: Competing ion effect and the mechanism analysis. Separation and Purification Technology, 2010, 76, 184-190.	7.9	141
14	Distributions of polycyclic aromatic hydrocarbons in the Daliao River Estuary of Liaodong Bay, Bohai Sea (China). Marine Pollution Bulletin, 2009, 58, 818-826.	5.0	130
15	Distribution and contamination assessment of heavy metals in sediment of the Second Songhua River, China. Environmental Monitoring and Assessment, 2008, 137, 329-342.	2.7	121
16	Calculation and application of Sb toxicity coefficient for potential ecological risk assessment. Science of the Total Environment, 2018, 610-611, 167-174.	8.0	112
17	Effects of different forms of antimony on rice during the period of germination and growth and antimony concentration in rice tissue. Science of the Total Environment, 1999, 243-244, 149-155.	8.0	108
18	Antimony(III) oxidation and antimony(V) adsorption reactions on synthetic manganite. Chemie Der Erde, 2012, 72, 41-47.	2.0	104

#	Article	IF	CITATIONS
19	Spatial and seasonal variations of antibiotics in river waters in the Haihe River Catchment in China and ecotoxicological risk assessment. Environment International, 2019, 130, 104919.	10.0	104
20	Catalytic oxidation of contaminants by FeO activated peroxymonosulfate process: Fe(IV) involvement, degradation intermediates and toxicity evaluation. Chemical Engineering Journal, 2020, 382, 123013.	12.7	103
21	A review of removal technology for antimony in aqueous solution. Journal of Environmental Sciences, 2020, 90, 189-204.	6.1	102
22	Distribution patterns of nitrobenzenes and polychlorinated biphenyls in water, suspended particulate matter and sediment from mid- and down-stream of the Yellow River (China). Chemosphere, 2006, 65, 365-374.	8.2	101
23	Distribution and sources of organochlorine pesticides in water and sediments from Daliao River estuary of Liaodong Bay, Bohai Sea (China). Estuarine, Coastal and Shelf Science, 2009, 84, 119-127.	2.1	101
24	Adsorption of antimony(V) on kaolinite as a function of pH, ionic strength and humic acid. Environmental Earth Sciences, 2010, 60, 715-722.	2.7	97
25	Distribution, partitioning and sources of polycyclic aromatic hydrocarbons in Daliao River water system in dry season, China. Journal of Hazardous Materials, 2009, 164, 1379-1385.	12.4	91
26	Antimony smelting process generating solid wastes and dust: Characterization and leaching behaviors. Journal of Environmental Sciences, 2014, 26, 1549-1556.	6.1	87
27	A Comprehensive Clobal Inventory of Atmospheric Antimony Emissions from Anthropogenic Activities, 1995–2010. Environmental Science & Technology, 2014, 48, 10235-10241.	10.0	87
28	The chemical, toxicological and ecological studies in assessing the heavy metal pollution in Le An River, China. Water Research, 1998, 32, 510-518.	11.3	85
29	Occurrence, spatiotemporal variation, and ecological risk of antibiotics in the water of the semi-enclosed urbanized Jiaozhou Bay in eastern China. Water Research, 2020, 184, 116187.	11.3	83
30	Aliphatic and polycyclic aromatic hydrocarbons in the Xihe River, an urban river in China's Shenyang City: Distribution and risk assessment. Journal of Hazardous Materials, 2011, 186, 1193-1199.	12.4	74
31	Anthropogenic Atmospheric Emissions of Antimony and Its Spatial Distribution Characteristics in China. Environmental Science & amp; Technology, 2012, 46, 3973-3980.	10.0	74
32	Adsorption of antimony(III) on goethite in the presence of competitive anions. Journal of Geochemical Exploration, 2013, 132, 201-208.	3.2	71
33	Background, baseline, normalization, and contamination of heavy metals in the Liao River Watershed sediments of China. Journal of Asian Earth Sciences, 2013, 73, 87-94.	2.3	68
34	Characterization of humic acids extracted from the sediments of the various rivers and lakes in China. Journal of Environmental Sciences, 2008, 20, 1294-1299.	6.1	65
35	Concentration and speciation of antimony and arsenic in soil profiles around the world's largest antimony metallurgical area in China. Environmental Geochemistry and Health, 2015, 37, 21-33.	3.4	65
36	Rapid photooxidation of Sb(III) in the presence of different Fe(III) species. Geochimica Et Cosmochimica Acta, 2016, 180, 214-226.	3.9	63

#	Article	IF	CITATIONS
37	Mechanisms of Sb(III) Photooxidation by the Excitation of Organic Fe(III) Complexes. Environmental Science & Technology, 2016, 50, 6974-6982.	10.0	63
38	Influence of combined pollution of antimony and arsenic on culturable soil microbial populations and enzyme activities. Ecotoxicology, 2011, 20, 9-19.	2.4	62
39	pH-dependent release characteristics of antimony and arsenic from typical antimony-bearing ores. Journal of Environmental Sciences, 2016, 44, 171-179.	6.1	61
40	Estrogens in municipal wastewater and receiving waters in the Beijing-Tianjin-Hebei region, China: Occurrence and risk assessment of mixtures. Journal of Hazardous Materials, 2020, 389, 121891.	12.4	59
41	Efficient removal of acetochlor pesticide from water using magnetic activated carbon: Adsorption performance, mechanism, and regeneration exploration. Science of the Total Environment, 2021, 778, 146353.	8.0	57
42	Monitoring and Assessment of Persistent Organochlorine Residues in Sediments from the Daliaohe River Watershed, Northeast of China. Environmental Monitoring and Assessment, 2007, 133, 231-242.	2.7	56
43	Activation of peroxymonosulfate by magnetic catalysts derived from drinking water treatment residuals for the degradation of atrazine. Journal of Hazardous Materials, 2019, 366, 402-412.	12.4	54
44	Kinetics and Mechanism of Photopromoted Oxidative Dissolution of Antimony Trioxide. Environmental Science & Technology, 2014, 48, 14266-14272.	10.0	53
45	Distribution, sources, and ecological risks of potentially toxic elements in the Laizhou Bay, Bohai Sea: Under the long-term impact of the Yellow River input. Journal of Hazardous Materials, 2021, 413, 125429.	12.4	52
46	The leaching characteristics and changes in the leached layer of antimony-bearing ores from China. Journal of Geochemical Exploration, 2017, 176, 76-84.	3.2	50
47	Dynamic flows of polyethylene terephthalate (PET) plastic in China. Waste Management, 2021, 124, 273-282.	7.4	49
48	Phosphorus sorption and fraction characteristics in the upper, middle and low reach sediments of the Daliao river systems, China. Journal of Hazardous Materials, 2009, 170, 278-285.	12.4	48
49	Occurrence, spatiotemporal distribution, and ecological risks of organophosphate esters in the water of the Yellow River to the Laizhou Bay, Bohai Sea. Science of the Total Environment, 2021, 787, 147528.	8.0	48
50	Spatiotemporal distribution, source, and ecological risk of polycyclic aromatic hydrocarbons (PAHs) in the urbanized semi-enclosed Jiaozhou Bay, China. Science of the Total Environment, 2020, 717, 137224.	8.0	47
51	Spatial and temporal patterns of acidity and heavy metals in predicting the potential for ecological impact on the Le An river polluted by acid mine drainage. Science of the Total Environment, 1997, 206, 67-77.	8.0	46
52	Temporal and spatial distribution of atmospheric antimony emission inventories from coal combustion in China. Environmental Pollution, 2011, 159, 1613-1619.	7.5	46
53	Phosphorus distribution in the estuarine sediments of the Daliao river, China. Estuarine, Coastal and Shelf Science, 2009, 84, 246-252.	2.1	44
54	Photopromoted oxidative dissolution of stibnite. Applied Geochemistry, 2015, 61, 53-61.	3.0	44

#	Article	IF	CITATIONS
55	Sources, trophodynamics, contamination and risk assessment of toxic metals in a coastal ecosystem by using a receptor model and Monte Carlo simulation. Journal of Hazardous Materials, 2022, 424, 127482.	12.4	43
56	Comparison of diffusive gradients in thin-films (DGT) and chemical extraction methods for predicting bioavailability of antimony and arsenic to maize. Geoderma, 2018, 332, 1-9.	5.1	42
57	Comparative sorption of benzo[î±]phrene to different humic acids and humin in sediments. Journal of Hazardous Materials, 2009, 166, 802-809.	12.4	41
58	Bacterial community profile of contaminated soils in a typical antimony mining site. Environmental Science and Pollution Research, 2018, 25, 141-152.	5.3	41
59	In situ measurements of concentrations of Cd, Co, Fe and Mn in estuarine porewater using DGT. Environmental Pollution, 2011, 159, 1123-1128.	7.5	40
60	Distribution and speciation of four heavy metals (Cd, Cr, Mn and Ni) in the surficial sediments from estuary in daliao river and yingkou bay. Environmental Earth Sciences, 2011, 63, 163-175.	2.7	39
61	Occurrence, migration, and allocation of arsenic in multiple media of a typical semi-enclosed bay. Journal of Hazardous Materials, 2020, 384, 121313.	12.4	39
62	Dynamic flow and pollution of antimony from polyethylene terephthalate (PET) fibers in China. Science of the Total Environment, 2021, 771, 144643.	8.0	39
63	Toxicity and bioavailability of antimony in edible amaranth (Amaranthus tricolor Linn.) cultivated in two agricultural soil types. Environmental Pollution, 2020, 257, 113642.	7.5	36
64	Contamination and ecological risk assessment of toxic trace elements in the Xi River, an urban river of Shenyang city, China. Environmental Monitoring and Assessment, 2013, 185, 4321-4332.	2.7	35
65	Uptake, translocation and phytotoxicity of antimonite in wheat (Triticum aestivum). Science of the Total Environment, 2019, 669, 421-430.	8.0	34
66	Responses of soil fungal and archaeal communities to environmental factors in an ongoing antimony mine area. Science of the Total Environment, 2019, 652, 1030-1039.	8.0	33
67	Effects of temperature and surfactants on naphthalene and phenanthrene sorption by soil. Journal of Environmental Sciences, 2009, 21, 667-674.	6.1	31
68	Distributions of polychlorinated biphenyls in the Daliao River estuary of Liaodong Bay, Bohai Sea (China). Marine Pollution Bulletin, 2014, 78, 77-84.	5.0	31
69	A bibliometric analysis of global research progress on pharmaceutical wastewater treatment during 1994–2013. Environmental Earth Sciences, 2015, 73, 4995-5005.	2.7	31
70	Anthropogenic antimony flow analysis and evaluation in China. Science of the Total Environment, 2019, 683, 659-667.	8.0	31
71	Effects of antimony (III/V) on microbial activities and bacterial community structure in soil. Science of the Total Environment, 2021, 789, 148073.	8.0	31
72	Degradation of simazine by heat-activated peroxydisulfate process: A coherent study on kinetics, radicals and models. Chemical Engineering Journal, 2021, 426, 131876.	12.7	31

#	Article	IF	CITATIONS
73	Antimony leaching release from brake pads: Effect of pH, temperature and organic acids. Journal of Environmental Sciences, 2015, 29, 11-17.	6.1	30

Element remobilization, $\hat{a} \in \hat{c}$ internal P-loading, $\hat{a} \in \hat{c}$ and sediment-P reactivity researched by DGT (diffusive) Tj ETQq0 0.0 rgBT $\frac{1}{30}$ verlock 1

75	Adsorption of antimony on kaolinite as a function of time, pH, HA and competitive anions. Environmental Earth Sciences, 2016, 75, 1.	2.7	30
76	Activation of peroxymonosulfate by WTRs-based iron-carbon composites for atrazine removal: Performance evaluation, mechanism insight and byproduct analysis. Chemical Engineering Journal, 2021, 421, 127811.	12.7	30
77	Contents, Enrichment, Toxicity and Baselines of trace elements in the estuarine and coastal sediments of the Daliao River System, China. Geochemical Journal, 2012, 46, 371-380.	1.0	29
78	Endocrine-disrupting chemicals in a typical urbanized bay of Yellow Sea, China: Distribution, risk assessment, and identification of priority pollutants. Environmental Pollution, 2021, 287, 117588.	7.5	29
79	Distribution, source, and ecological risks of polycyclic aromatic hydrocarbons in Lake Qinghai, China. Environmental Pollution, 2020, 266, 115401.	7.5	28
80	Profiling of the spatiotemporal distribution, risks, and prioritization of antibiotics in the waters of Laizhou Bay, northern China. Journal of Hazardous Materials, 2022, 424, 127487.	12.4	28
81	Distribution, partitioning, and health risk assessment of organophosphate esters in a major tributary of middle Yangtze River using Monte Carlo simulation. Water Research, 2022, 219, 118559.	11.3	28
82	Organic ligand-induced dissolution kinetics of antimony trioxide. Journal of Environmental Sciences, 2017, 56, 87-94.	6.1	27
83	Activation of peroxymonosulfate using drinking water treatment residuals modified by hydrothermal treatment for imidacloprid degradation. Chemosphere, 2020, 254, 126820.	8.2	27
84	Modeling the ecological impact of heavy metals on aquatic ecosystems: a framework for the development of an ecological model. Science of the Total Environment, 2001, 266, 291-298.	8.0	25
85	Environmental impacts of heavy metals (Co, Cu, Pb, Zn) in surficial sediments of estuary in Daliao River and Yingkou Bay (northeast China): concentration level and chemical fraction. Environmental Earth Sciences, 2012, 66, 2417-2430.	2.7	25
86	Antimony adsorption on kaolinite in the presence of competitive anions. Environmental Earth Sciences, 2014, 71, 2989-2997.	2.7	25
87	Higher Fine Particle Fraction in Sediment Increased Phosphorus Flux to Estuary in Restored Yellow River Basin. Environmental Science & Technology, 2021, 55, 6783-6790.	10.0	25
88	Assessment of cadmium pollution and subsequent ecological and health risks in Jiaozhou Bay of the Yellow Sea. Science of the Total Environment, 2021, 774, 145016.	8.0	25
89	Interactions of antimony with biomolecules and its effects on human health. Ecotoxicology and Environmental Safety, 2022, 233, 113317.	6.0	25
90	Content, enrichment, and regional geochemical baseline of antimony in the estuarine sediment of the Daliao river system in China. Chemie Der Erde, 2012, 72, 23-28.	2.0	24

#	Article	IF	CITATIONS
91	Distribution and contamination assessment of toxic trace elements in sediment of the Daliao River System, China. Environmental Earth Sciences, 2013, 70, 3163-3173.	2.7	24
92	Removal of Sb(III) and Sb(V) from aqueous media by goethite. Water Quality Research Journal of Canada, 2013, 48, 223-231.	2.7	24
93	Distribution and Speciation of Selenium, Antimony, and Arsenic in Soils and Sediments Around the Area of Xikuangshan (China). Clean - Soil, Air, Water, 2016, 44, 1538-1546.	1.1	24
94	Changes in fertilizer categories significantly altered the estimates of ammonia volatilizations induced from increased synthetic fertilizer application to Chinese rice fields. Agriculture, Ecosystems and Environment, 2018, 265, 112-122.	5.3	24
95	Insight into removal of dissolved organic matter in post pharmaceutical wastewater by coagulation-UV/H2O2. Journal of Environmental Sciences, 2019, 76, 329-338.	6.1	24
96	Concentrations, fluxes, and potential sources of nitrogen and phosphorus species in atmospheric wet deposition of the Lake Qinghai Watershed, China. Science of the Total Environment, 2019, 682, 523-531.	8.0	24
97	Effect of dissolved organic matter on sorption and desorption of phenanthrene onto black carbon. Journal of Environmental Sciences, 2013, 25, 2378-2383.	6.1	23
98	Comparison of polycyclic aromatic hydrocarbons in sediments from the Songhuajiang River (China) during different sampling seasons. Journal of Environmental Science and Health - Part A Toxic/Hazardous Substances and Environmental Engineering, 2007, 42, 119-127.	1.7	22
99	Effect of structural variations on sorption and desorption of phenanthrene by sediment organic matter. Journal of Hazardous Materials, 2010, 184, 432-438.	12.4	22
100	Vanadium pollution and health risks in marine ecosystems: Anthropogenic sources over natural contributions. Water Research, 2021, 207, 117838.	11.3	22
101	Occurrence and risk assessment of total mercury and methylmercury in surface seawater and sediments from the Jiaozhou Bay, Yellow Sea. Science of the Total Environment, 2020, 714, 136539.	8.0	20
102	Antimonite oxidation and adsorption onto two tunnel-structured manganese oxides: Implications for antimony mobility. Chemical Geology, 2021, 579, 120336.	3.3	20
103	Trophic transfer and dietary exposure risk of mercury in aquatic organisms from urbanized coastal ecosystems. Chemosphere, 2021, 281, 130836.	8.2	20
104	Mercury Contamination and Dynamics in the Sediment of the Second Songhua River, China. Soil and Sediment Contamination, 2007, 16, 397-411.	1.9	19
105	Characteristics of petroleum hydrocarbons in surficial sediments from the Songhuajiang River (China): spatial and temporal trends. Environmental Monitoring and Assessment, 2011, 179, 81-92.	2.7	19
106	Adsorption of methylantimony and methylarsenic on soils, sediments, and mine tailings from antimony mine area. Microchemical Journal, 2015, 123, 158-163.	4.5	19
107	The measurement of metals by diffusive gradients in thin films (DGT) at sediment/water interface (SWI) of bay and remobilization assessment. Environmental Earth Sciences, 2015, 73, 6283-6295.	2.7	19
108	Organophosphate esters in surface waters of Shandong Peninsula in eastern China: Levels, profile, source, spatial distribution, and partitioning. Environmental Pollution, 2022, 297, 118792.	7.5	19

#	Article	IF	CITATIONS
109	Simultaneous stabilization of Sb and As co-contaminated soil by Fe Mg modified biochar. Science of the Total Environment, 2022, 830, 154831.	8.0	19
110	Comparison of the reaction kinetics and mechanisms of Sb(III) oxidation by reactive oxygen species from pristine and surface-oxidized pyrite. Chemical Geology, 2020, 552, 119790.	3.3	18
111	Facile co-removal of As(V) and Sb(V) from aqueous solution using Fe-Cu binary oxides: Structural modification and self-driven force field of copper oxides. Science of the Total Environment, 2022, 803, 150084.	8.0	18
112	Geochemical baseline and distribution of cobalt, manganese, and vanadium in the Liao River Watershed sediments of China. Geosciences Journal, 2013, 17, 455-464.	1.2	17
113	Mechanochemical treatment with CaO-activated PDS of HCB contaminated soils. Chemosphere, 2020, 257, 127207.	8.2	17
114	Influences of Particles and Aquatic Colloids on the Oxidation of Sb(III) in Natural Water. ACS Earth and Space Chemistry, 2020, 4, 661-671.	2.7	17
115	Toxicity and bioavailability of antimony to the earthworm (Eisenia fetida) in different agricultural soils. Environmental Pollution, 2021, 291, 118215.	7.5	17
116	Ecological status classification of the Taizi River Basin, China: a comparison of integrated risk assessment approaches. Environmental Science and Pollution Research, 2015, 22, 14738-14754.	5.3	16
117	Influence of Fe(II) on Sb(III) oxidation and adsorption by MnO2 under acidic conditions. Science of the Total Environment, 2020, 724, 138209.	8.0	16
118	Quantify phosphorus transport distinction of different reaches to estuary under long-term anthropogenic perturbation. Science of the Total Environment, 2021, 780, 146647.	8.0	16
119	Spatial-temporal characteristics of phosphorus in non-point source pollution with grid-based export coefficient model and geographical information system. Water Science and Technology, 2015, 71, 1709-1717.	2.5	15
120	Effect of organic matter on mobilization of antimony from nanocrystalline titanium dioxide. Environmental Technology (United Kingdom), 2018, 39, 1515-1521.	2.2	15
121	Trophodynamics of arsenic for different species in coastal regions of the Northwest Pacific Ocean: In situ evidence and a meta-analysis. Water Research, 2020, 184, 116186.	11.3	15
122	Insights into the spatiotemporal occurrence and mixture risk assessment of household and personal care products in the waters from rivers to Laizhou Bay, southern Bohai Sea. Science of the Total Environment, 2022, 810, 152290.	8.0	15
123	Adsorption behavior and surface complexation modeling of oxygen anion Sb(V) adsorption on goethite. Science of the Total Environment, 2022, 833, 155284.	8.0	15
124	Distribution, removal and chemical forms of heavy metals in polluted rice seed. Toxicological and Environmental Chemistry, 2000, 76, 137-145.	1.2	14
125	Determination of o-phthalic acid in snow and its photochemical degradation by capillary gas chromatography coupled with flame ionization and mass spectrometric detection. Chemosphere, 2011, 83, 1014-1019.	8.2	14
126	Influence of atmospheric surface oxidation on the formation of H2O2 and â^™OH at pyrite-water interface: Mechanism and kinetic model. Chemical Geology, 2021, 571, 120176.	3.3	14

#	Article	IF	CITATIONS
127	Seasonal occurrence, allocation and ecological risk of organophosphate esters in a typical urbanized semi-closed bay. Environmental Pollution, 2021, 290, 118074.	7.5	14
128	Rare earth element content in the SPM of Daliao river system and its comparison with that in the sediments, loess and soils in China. Journal of Rare Earths, 2008, 26, 414-420.	4.8	12
129	Biodegradation of polycyclic aromatic hydrocarbons in sediments from the Daliao River watershed, China. Journal of Environmental Sciences, 2009, 21, 865-871.	6.1	12
130	The distribution, sources and toxicity risks of polycyclic aromatic hydrocarbons and n-alkanes in riverine and estuarine core sediments from the Daliao River watershed. Environmental Earth Sciences, 2013, 68, 2015-2024.	2.7	12
131	Efficient catalyst prepared from water treatment residuals and industrial glucose using hydrothermal treatment: Preparation, characterization and its catalytic performance for activating peroxymonosulfate to degrade imidacloprid. Chemosphere, 2022, 290, 133326.	8.2	12
132	Chemical forms and ecological risk of arsenic in the sediment of the Daliao River System in China. Environmental Monitoring and Assessment, 2012, 184, 2237-2245.	2.7	11
133	Geochemical baseline level and function and contamination of phosphorus in Liao River Watershed sediments of China. Journal of Environmental Management, 2013, 128, 138-143.	7.8	11
134	Adsorption of Antimony on Sediments from Typical Water Systems in China: A Comparison of Sb(III) and Sb(V) Pattern. Soil and Sediment Contamination, 2014, 23, 37-48.	1.9	11
135	Substance flow analysis and environmental release of antimony in the life cycle of polyethylene terephthalate products. Journal of Cleaner Production, 2021, 291, 125252.	9.3	11
136	Description of microbial community structure of sediments from the Daliao River water system and its estuary (NE China) by application of fluorescence in situ hybridization. Environmental Earth Sciences, 2010, 61, 1725-1734.	2.7	10
137	Effect of Surfactants on Sorption and Desorption of Phenanthrene onto Black Carbon. Water Environment Research, 2011, 83, 15-22.	2.7	10
138	Distribution patterns of nitroaromatic compounds in the water, suspended particle and sediment of the river in a long-term industrial zone (China). Environmental Monitoring and Assessment, 2011, 177, 515-526.	2.7	10
139	Distribution of rare earth elements in the estuarine and coastal sediments of the Daliao River System, China. Journal of Radioanalytical and Nuclear Chemistry, 2013, 298, 627-634.	1.5	10
140	The assessment of localized remobilization and geochemical process of 14 metals at sediment/water interface (SWI) of Yingkou coast (China) by diffusive gradients in thin films (DGT). Environmental Earth Sciences, 2015, 73, 6081-6090.	2.7	10
141	Comparison of masking agents for antimony speciation analysis using hydride generation atomic fluorescence spectrometry. Frontiers of Environmental Science and Engineering, 2015, 9, 970-978.	6.0	10
142	Simultaneous electrochemical determination of Sb(III) and Sb(V) in Water samples: Deposition potential differences and Sb(III) photooxidation characteristics. Sensors and Actuators B: Chemical, 2020, 305, 127454.	7.8	10
143	Response of soil microbial activities and ammonia oxidation potential to environmental factors in a typical antimony mining area. Journal of Environmental Sciences, 2023, 127, 767-779.	6.1	10
144	THE PATTERNS OF Cd-BINDING PROTEINS IN RICE AND WHEAT SEED AND THEIR STABILITY. Journal of Environmental Science and Health - Part A Toxic/Hazardous Substances and Environmental Engineering, 2002, 37, 541-551.	1.7	9

MENG-CHANG HE

#	Article	IF	CITATIONS
145	Phosphorus content and fractionation of phosphate in the surface sediments of the Daliao river system in China. Environmental Earth Sciences, 2010, 59, 1349-1357.	2.7	9
146	Phenanthrene sorption to humic acids, humin, and black carbon in sediments from typical water systems in China. Environmental Monitoring and Assessment, 2010, 166, 445-459.	2.7	9
147	Transcriptomic Profiles in Zebrafish Liver Permit the Discrimination of Surface Water with Pollution Gradient and Different Discharges. International Journal of Environmental Research and Public Health, 2018, 15, 1648.	2.6	9
148	Predicted models for phenanthrene sorption nonlinearity and capacity based on different HA/BC ratios in sediments. Journal of Colloid and Interface Science, 2009, 337, 338-344.	9.4	8
149	Behavior of stabilized multiwalled carbon nanotubes in a FeCl3 coagulation system and the structure characteristics of the produced flocs. Journal of Colloid and Interface Science, 2012, 366, 173-178.	9.4	8
150	Speciation of Antimony in Soils and Sediments by Liquid Chromatography–Hydride Generation–Atomic Fluorescence Spectrometry. Analytical Letters, 2015, 48, 1941-1953.	1.8	8
151	Anthropogenic and lithogenic fluxes of atmospheric lead deposition over the past 3600 years from a peat bog, Changbai Mountains, China. Chemosphere, 2019, 227, 225-236.	8.2	8
152	Mechanism of birnessite-promoted oxidative dissolution of antimony trioxide. Environmental Chemistry, 2020, 17, 345.	1.5	8
153	Occurrence of Aliphatic Hydrocarbons in Water, Suspended Particulate Matter and Sediments of Daliao River System, China. Bulletin of Environmental Contamination and Toxicology, 2010, 84, 519-523.	2.7	7
154	Synergetic loss of heavy metal and phosphorus: Evidence from geochemical fraction and estuary sedimentation. Journal of Hazardous Materials, 2021, 416, 125710.	12.4	7
155	Insight into the Sb(III) and Sb(V) removal mechanisms on porous Fe-Ti-chitosan composite: Experiment and DFT calculations. Chemical Engineering Journal, 2022, 432, 134420.	12.7	7
156	Distribution and proteinâ€binding forms of heavy metals in polluted wheat seed. Journal of Environmental Science and Health - Part A Toxic/Hazardous Substances and Environmental Engineering, 2000, 35, 1891-1899.	1.7	6
157	DISTRIBUTION OF PERSISTENT ORGANOCHLORINE RESIDUES IN SEDIMENTS FROM THE SONGHUAJIANG RIVER, NORTHEAST CHINA. Environmental Technology (United Kingdom), 2008, 29, 303-314.	2.2	6
158	Comparative Sorption of Phenanthrene and Benzo $[\hat{l}\pm]$ pyrene to Soil Humic Acids. Soil and Sediment Contamination, 2009, 18, 725-738.	1.9	6
159	Sorption dynamics, geochemical fraction and driving factors in phosphorus transport at large basin scale. Journal of Cleaner Production, 2021, 294, 126111.	9.3	6
160	Baseline, enrichment, and ecological risk of arsenic and antimony in the Jiaozhou Bay, a semi-enclosed bay of the Yellow Sea, China. Marine Pollution Bulletin, 2021, 168, 112431.	5.0	6
161	Microbial community structure and metabolic potential in the coastal sediments around the Yellow River Estuary. Science of the Total Environment, 2022, 816, 151582.	8.0	6
162	Horizontal planetary mechanochemical method for rapid and efficient remediation of high-concentration lindane-contaminated soils in an alkaline environment. Journal of Hazardous Materials, 2022, 436, 129078.	12.4	6

MENG-CHANG HE

#	Article	IF	CITATIONS
163	Application of the Export Coefficient Model in Estimating Nutrient Pollution of Dahuofang Reservoir Drainage Basin, Daliao River, China. , 2008, , .		5
164	Effects of different sediment fractions on sorption of galaxolide. Frontiers of Environmental Science and Engineering, 2012, 6, 59-65.	6.0	5
165	Arsenic Distribution and Adsorption Behavior in the Sediments of the Daliao River System in China. Water Environment Research, 2013, 85, 687-695.	2.7	5
166	Thermodynamic Assessment of Effects of Solution Conditions on Precipitation and Recovery of Phosphorus from Wastewater. Environmental Engineering Science, 2015, 32, 574-581.	1.6	5
167	Quantitative source identification and environmental assessment of trace elements in the water and sediment of rivers flowing into Laizhou Bay, Bohai Sea. Marine Pollution Bulletin, 2022, 174, 113313.	5.0	5
168	Historical records of trace metals in two sediment cores of Jiaozhou Bay, north China. Marine Pollution Bulletin, 2022, 175, 113400.	5.0	5
169	Simultaneous removal of antimony and arsenic by nano-TiO ₂ -crosslinked chitosan (TA-chitosan) beads. Environmental Technology (United Kingdom), 2023, 44, 2913-2923.	2.2	5
170	Deep insight into the Sb(III) and Sb(V) removal mechanism by Fe–Cu-chitosan material. Environmental Pollution, 2022, 303, 119160.	7.5	5
171	Enrichment and Chemical Fraction of Copper and Zinc in the Sediments of the Daliao River System, China. Soil and Sediment Contamination, 2009, 18, 688-701.	1.9	4
172	Effect of Combined <i>Bacillus subtilis</i> on the Sorption of Phenanthrene and 1,2,3â€Trichlorobenzene onto Mineral Surfaces. Journal of Environmental Quality, 2010, 39, 236-244.	2.0	4
173	Norfloxacin Sorption to Different Fractions in Sediments from Typical Water Systems in China. Soil and Sediment Contamination, 2011, 20, 564-580.	1.9	4
174	High-resolution profiles of iron, manganese, cobalt, cadmium, copper and zinc in the pore water of estuarine sediment. International Journal of Environmental Science and Technology, 2013, 10, 275-282.	3.5	4
175	Spatiotemporal variations in phosphorus concentrations in the water and sediment of Jiaozhou Bay and sediment phosphorus release potential. Science of the Total Environment, 2022, 806, 150540.	8.0	4
176	Oxidation and adsorption of Sb(III) in the presence of iron (hydr)oxides and dissolved Mn(II). Chemical Geology, 2022, 591, 120725.	3.3	4
177	Foreword to the Special Issue on â€~Antimony in the Environment: A Chinese Perspective'. Environmental Chemistry, 2020, 17, 303.	1.5	3
178	Continuous removal of aromatic hydrocarbons by an AF reactor under denitrifying conditions. World Journal of Microbiology and Biotechnology, 2007, 23, 1711-1717.	3.6	2
179	Heavy metal contamination in the sediment of the Second Songhua River. Diqiu Huaxue, 2006, 25, 118-119.	0.5	1
180	Distribution of Microbial Community in the Sediments of the Daliao River Water System, China. , 2009,		0

0

#	Article	IF	CITATIONS
181	Phenanthrene sorption to environmental black carbon in sediments from the Song-Liao watershed (China). Frontiers of Environmental Science and Engineering in China, 2009, 3, 434-442.	0.8	0

Antimony, Arsenic and Other Toxic Elements in the Topsoil of an Antimony Mine Area., 2010, , 58-61.